
Modeling Heterogeneous Hierarchies with Relation-specific Hyperbolic Cones

Yushi Bai*

bys18@mails.tsinghua.edu.cn
Tsinghua University

Rex Ying*

rexying@stanford.edu
Stanford University

Hongyu Ren

hyren@cs.stanford.edu
Stanford University

Jure Leskovec

jure@cs.stanford.edu
Stanford University

Abstract

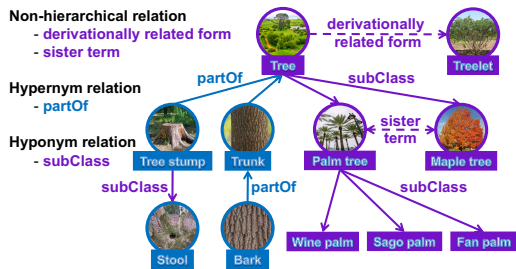
Hierarchical relations are prevalent and indispensable for organizing human knowledge captured by a knowledge graph (KG). The key property of hierarchical relations is that they induce a partial ordering over the entities, which needs to be modeled in order to allow for hierarchical reasoning. However, current KG embeddings can model only a single global hierarchy (single global partial ordering) and fail to model multiple heterogeneous hierarchies that exist in a single KG. Here we present ConE (Cone Embedding), a KG embedding model that is able to simultaneously model multiple hierarchical as well as non-hierarchical relations in a knowledge graph. ConE embeds entities into hyperbolic cones and models relations as transformations between the cones. In particular, ConE uses cone containment constraints in different subspaces of the hyperbolic embedding space to capture multiple heterogeneous hierarchies. Experiments on standard knowledge graph benchmarks show that ConE obtains state-of-the-art performance on hierarchical reasoning tasks as well as knowledge graph completion task on hierarchical graphs. In particular, our approach yields new state-of-the-art Hits@1 of 45.3% on WN18RR and 16.1% on DDB14 (0.231 MRR). As for hierarchical reasoning task, our approach outperforms previous best results by an average of 20% across three hierarchical datasets.

1 Introduction

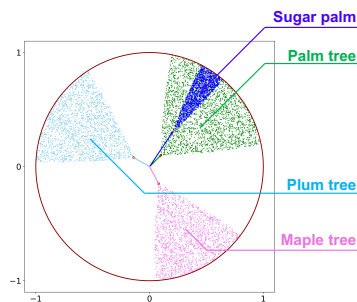
Knowledge graph (KG) is a prevalent data structure that stores factual knowledge in the form of triplets, which connect two entities (nodes) with a relation (edge) [1]. Knowledge graphs play an important role in many scientific and machine learning applications, including question answering [2], information retrieval [3] and discovery in biomedicine [4]. Knowledge graph completion is the problem of predicting missing relations in the graph, and is crucial in many real-world applications. Knowledge graph embedding (KGE) models [5, 6, 7] approach the task by embedding entities and relations into low-dimensional vector space and then use the embeddings to learn a function that given a head entity h and a relation r predicts the tail entity t .

Hierarchical information is ubiquitous in real-world KGs, such as WordNet [8] or Gene Ontology [9], since much human knowledge is organized hierarchically. The relations in these KGs can be separated into non-hierarchical relations (e.g., *likes*, *friendOf*) and hierarchical relations (e.g., *isA*,

*Equal contribution



(a) Multiple heterogeneous hierarchies in knowledge graph.



(b) Hyperbolic entailment cones in 2D hyperbolic plane for $K = 0.1$.

Figure 1: (a) There are three categories of relations: non-hierarchical relation (*sister term*), hypernym (*partOf*) and hyponym relation (*subClass*). Relations induce multiple independent hierarchies. (b) ConE uses d 2D hyperbolic entailment cones to model an entity. Entities *PalmTree* and *SugarPalm* are connected by a hyponym relation *subClass* and therefore the cone of *PalmTree* contains the cone of *SugarPalm*.

partOf), where non-hierarchical relations capture interactions between the entities at the same level while hierarchical relations induce a tree-like partial ordering structure of entities.

Recent works propose the use of a variety of embedding geometries such as hyperbolic embeddings, box embeddings, and cone embeddings [10, 11, 12] to model partial ordering property of hierarchical relations, but two important challenges remain: **(1)** Existing works that consider hierarchical relations [13] do not take into account existing non-hierarchical relations [14]. **(2)** These methods can only be applied to graphs with a single hierarchical relation type, and are thus not suitable to real-world knowledge graphs that simultaneously encode multiple hierarchies using many different relations. For example, in Figure 1, *subClass* and *partOf* each define a unique hierarchy over the same set of entities. However, existing models treat all relations in a KG as part of one single hierarchy, limiting the ability to reason with different types of heterogeneous hierarchical relations. While there are methods for reasoning over KGs that use hyperbolic space (MuRP [15], RotH [16]), which is suitable for modeling tree-like graphs, the choice of relational transformations used in these works (rotation) prevents them from faithfully capturing all the properties of hierarchical relations. For example, they cannot model transitivity of hierarchical relations: if there exist triplets (h_1, r, h_2) and (h_2, r, h_3) , then (h_1, r, h_3) exists, *i.e.* h_1 and h_3 are also related by relation r .

Here we propose a novel hyperbolic knowledge graph embedding model ConE. ConE is motivated by the transitivity of nested angular cones [12] that naturally model the partial ordering defined by hierarchical relations. Our proposed approach embeds entities into the product space of hyperbolic planes, where the coordinate in each hyperbolic plane corresponds to a 2D hyperbolic cone. To address challenge **(1)**, we model non-hierarchical relations as hyperbolic cone rotations from head entity to tail entity, while we model hierarchical relations as a restricted rotation which guarantees cone containment (Figure 1(b)). To address challenge **(2)**, we assign distinct embedding subspaces corresponding to product spaces of a different set of hyperbolic planes for each hierarchical relation, to enforce cone containment constraints. By doing so, multiple heterogeneous hierarchies are preserved simultaneously in unique subspaces, allowing ConE to perform multiple hierarchical reasoning tasks accurately.

We evaluate the performance of ConE on the KG completion task and hierarchical reasoning task. A single trained ConE model can achieve remarkable performance on both tasks simultaneously. On KG completion task, ConE achieves new state-of-the-art results on two benchmark knowledge graph datasets including WN18RR [5, 17], DDB14 [18] (outperforming by **0.9%** and **4.5%** on Hits@1 metric). We also develop a novel biological knowledge graph GO21 from biomedical domain and show that ConE successfully models multiple hierarchies induced by different biological processes. We also evaluate our model against previous hierarchical modeling approaches on ancestor-descendant prediction task. Results show that ConE significantly outperforms baseline models (by **20%** on average when missing links are included), suggesting that it effectively models multiple

heterogeneous hierarchies. Moreover, ConE performs well on the lowest common ancestor (LCA) prediction task, improving over previous methods by **100%** in Hits@3 metric.

2 Related Work

Hierarchical reasoning. The most related line of work is learning structured embeddings to perform hierarchical reasoning on graphs and ontologies: order embedding, probabilistic order embedding, box embedding, Gumbel-box embedding and hyperbolic embedding [10, 11, 12, 19, 20, 21, 22]. These embedding-based methods map entities to various geometric representations that can capture the transitivity and entailment of hierarchical relations. These methods aim to perform hierarchical reasoning (transitive closure completion), such as predicting if an entity is an ancestor of another entity. However, the limitation of the above works is that they can only model a single hierarchical relation, and it remains unexplored how to extend them to multiple hierarchical relations in heterogeneous knowledge graphs. Recently, [23] builds upon the box embedding and further models joint (two) hierarchies using two boxes as entity embeddings. However, the method is not scalable since the model needs to learn a quadratic number of transformation functions between all pairs of hierarchical relations. Furthermore, the missing part is that these methods do not leverage non-hierarchical relations to further improve the hierarchy modeling. For example in Figure 1(a), with the *sisterTerm(PalmTree, MapleTree)* and *subClass(PalmTree, Tree)*, we may infer *subClass(MapleTree, Tree)*. In contrast to prior methods, ConE is able to achieve exactly this type of reasoning as it can simultaneously model multiple hierarchical as well as non-hierarchical relations.

Knowledge graph embedding. Various embedding methods have been proposed to model entities and relations in heterogeneous knowledge graphs. Prominent examples include TransE [5], DistMult [24], ComplEx [25], RotatE [7] and TuckER [14]. These methods often require high embedding dimensionality to model all the triples. Recently KG embeddings based on hyperbolic space have shown success in modeling hierarchical knowledge graphs. MuRP [15] learns relation-specific parameters in the Poincaré ball model. RotH [16] uses rotation and reflection transformation in n -dimensional Poincaré space to model relational patterns, and achieves state-of-the-art for the KG completion task, especially under low-dimensionality. However, transformations used in MuRP and RotH cannot capture transitive relations which hierarchical relations naturally are.

To the best of our knowledge, ConE is the first model that can faithfully model multiple hierarchical as well as non-hierarchical relations in a single embedding framework.

3 ConE Model Framework

3.1 Preliminaries

Knowledge graphs and knowledge graph embeddings. We denote the entity set and the relation set in knowledge graph as \mathcal{E} and \mathcal{R} respectively. Each edge in the graph is represented by a triplet (h, r, t) , connecting the head entity $h \in \mathcal{E}$ and the tail entity $t \in \mathcal{E}$ with relation $r \in \mathcal{R}$. In KG embedding models, entities and relations are mapped to vectors: $\mathcal{E} \rightarrow \mathbb{R}^{d_{\mathcal{E}}}$, $\mathcal{R} \rightarrow \mathbb{R}^{d_{\mathcal{R}}}$. Here $d_{\mathcal{E}}, d_{\mathcal{R}}$ refer to the dimensionality of entity and relation embeddings, respectively. Specifically, the mapping is learnt via optimizing a defined scoring function $\mathbb{R}^{d_{\mathcal{E}}} \times \mathbb{R}^{d_{\mathcal{R}}} \times \mathbb{R}^{d_{\mathcal{E}}} \rightarrow \mathbb{R}$ measuring the likelihood of triplets [16], while maximizing such likelihood only for true triplets.

Hierarchies in knowledge graphs. Many real-world knowledge graphs contain hierarchical relations [10, 11, 26]. Such hierarchical structure is characterized by very few top-level nodes corresponding to general and abstract concepts and a vast number of bottom-level nodes corresponding to concrete instances or components of the concept. Examples of hierarchical relations include *isA*, *partOf*. Note that there may exist multiple (heterogeneous) hierarchical relations in the same graph, which induce several different potentially incompatible hierarchies (i.e., partial orderings) over the same set of entities (Figure 1(a)). In contrast to prior work, our approach is able to model many simultaneous hierarchies over the same set of entities.

Hyperbolic embeddings. Hyperbolic embeddings can naturally capture hierarchical structures. Hyperbolic geometry is a non-Euclidean geometry with a constant negative curvature, where curvature measures how a geometric manifold deviates from Euclidean space. In this work, we use Poincaré ball model with constant curvature $c = -1$ as the hyperbolic space for entity embeddings [10].

We also investigate on more flexible curvatures, see Appendix B, results show that our model is robust enough with constant curvature $c = -1$. In particular, we denote d -dimensional Poincaré ball centered at origin as $\mathcal{B}^d = \{\mathbf{x} \in \mathbb{R}^d : \|\mathbf{x}\| < 1\}$, where $\|\cdot\|$ is the Euclidean norm. The Poincaré ball model of hyperbolic space is equipped with Riemannian metric:

$$g^{\mathcal{B}} = \left(\frac{2}{1 - \|\mathbf{x}\|^2}\right)^2 g^E \quad (1)$$

where g^E denotes the Euclidean metric, i.e., $g^E = \mathbf{I}_d$. The mobius addition \oplus [27] defined on Poincaré ball model with -1 curvature is given by:

$$\mathbf{x} \oplus \mathbf{y} = \frac{(1 + 2\langle \mathbf{x}, \mathbf{y} \rangle + \|\mathbf{y}\|^2)\mathbf{x} + (1 - \|\mathbf{x}\|^2)\mathbf{y}}{1 + 2\langle \mathbf{x}, \mathbf{y} \rangle + \|\mathbf{x}\|^2 \|\mathbf{y}\|^2} \quad (2)$$

For each point $\mathbf{x} \in \mathcal{B}^d$, the tangent space $\mathcal{T}_{\mathbf{x}}\mathcal{B}$ is the Euclidean vector space containing all tangent vectors at \mathbf{x} . One can map vectors in $\mathcal{T}_{\mathbf{x}}\mathcal{B}$ to vectors in \mathcal{B}^d through exponential map $\exp_{\mathbf{x}}(\cdot) : \mathcal{T}_{\mathbf{x}}\mathcal{B} \rightarrow \mathcal{B}^d$ as follows:

$$\exp_{\mathbf{x}}(\mathbf{u}) = \mathbf{x} \oplus \tanh\left(\frac{\|\mathbf{u}\|}{1 - \|\mathbf{x}\|}\right) \frac{\mathbf{u}}{\|\mathbf{u}\|} \quad (3)$$

Conversely, the logarithmic map $\log_{\mathbf{x}}(\cdot) : \mathcal{B}^d \rightarrow \mathcal{T}_{\mathbf{x}}\mathcal{B}$ maps vectors in \mathcal{B}^d back to vectors in $\mathcal{T}_{\mathbf{x}}\mathcal{B}$, in particular:

$$\log_{\mathbf{x}}(\mathbf{u}) = (1 - \|\mathbf{x}\|) \cdot \tanh^{-1}\left(\frac{\|\mathbf{u}\|}{1 - \|\mathbf{x}\|}\right) \frac{-\mathbf{x} \oplus \mathbf{u}}{\|-\mathbf{x} \oplus \mathbf{u}\|} \quad (4)$$

Also, the hyperbolic distance between $\mathbf{x}, \mathbf{y} \in \mathcal{B}^d$ is:

$$d_{\mathcal{B}}(\mathbf{x}, \mathbf{y}) = 2 \tanh^{-1}(\|-\mathbf{x} \oplus \mathbf{y}\|) \quad (5)$$

A key property of hyperbolic space is that the amount of space covered by a ball of radius r in hyperbolic space increases exponentially with respect to r , rather than polynomially as in Euclidean space. This property contributes to the fact that hyperbolic space can naturally model hierarchical tree-like structure.

Hyperbolic entailment cones. Each hierarchical relation induces a partial ordering over the entities. To capture a given partial ordering, we use the hyperbolic entailment cones [12]. Figure 1(b) gives an example of 2D hyperbolic cones.

Let $\mathcal{C}_{\mathbf{x}}$ denotes the cone at apex \mathbf{x} . The goal is to model partial order by containment relationship between cones, in particular, the entailment cones satisfy transitivity:

$$\forall \mathbf{x}, \mathbf{y} \in \mathcal{B}^d \setminus \{\mathbf{0}\} : \mathbf{y} \in \mathcal{C}_{\mathbf{x}} \Rightarrow \mathcal{C}_{\mathbf{y}} \subseteq \mathcal{C}_{\mathbf{x}} \quad (6)$$

Also, for $\mathbf{x}, \mathbf{y} \in \mathcal{B}^d$, we define the angle of \mathbf{y} at \mathbf{x} to be the angle between the half-lines $\overrightarrow{\mathbf{ox}}$ and $\overrightarrow{\mathbf{xy}}$ and denote it as $\angle_{\mathbf{x}}\mathbf{y}$. It can be expressed as:

$$\angle_{\mathbf{x}}\mathbf{y} = \cos^{-1}\left(\frac{\langle \mathbf{x}, \mathbf{y} \rangle (1 + \|\mathbf{x}\|^2) - \|\mathbf{x}\|^2 (1 + \|\mathbf{y}\|^2)}{\|\mathbf{x}\| \|\mathbf{x} - \mathbf{y}\| \sqrt{1 + \|\mathbf{x}\|^2 \|\mathbf{y}\|^2 - 2\langle \mathbf{x}, \mathbf{y} \rangle}}\right) \quad (7)$$

To satisfy transitivity of nested angular cones and symmetric conditions [12], we have the following expression of Poincaré entailment cone at apex $\mathbf{x} \in \mathcal{B}^d$:

$$\mathcal{C}_{\mathbf{x}} = \{\mathbf{y} \in \mathcal{B}^d \mid \angle_{\mathbf{x}}\mathbf{y} \leq \sin^{-1}\left(K \frac{1 - \|\mathbf{x}\|^2}{\|\mathbf{x}\|}\right)\} \quad (8)$$

where $K \in \mathbb{R}$ is a hyperparameter (we take $K = 0.1$). This implies that the half aperture $\phi_{\mathbf{x}}$ of cone $\mathcal{C}_{\mathbf{x}}$ is as follows:

$$\phi_{\mathbf{x}} = \sin^{-1}\left(K \frac{1 - \|\mathbf{x}\|^2}{\|\mathbf{x}\|}\right) \quad (9)$$

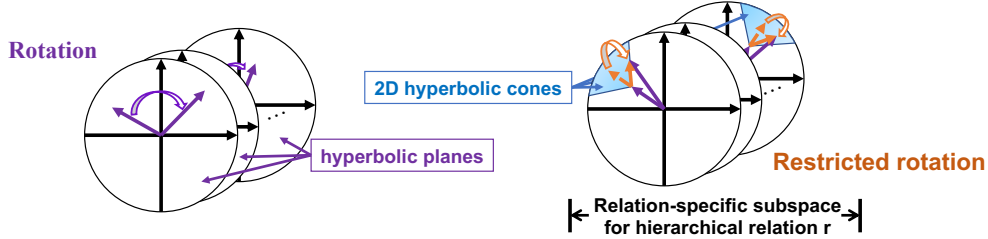


Figure 2: ConE model overview: Embedding space is the product space of d hyperbolic planes and ConE learns a different transformation in each hyperbolic plane. ConE uses **restricted rotation** in an assigned relation-specific subspace to model each hierarchical relation r and enforces cone containment constraint in the subspace so that partial ordering of cones is preserved in the subspace. For hyperbolic planes not in the subspace, we use a general **rotation** to model r . How to choose a relation-specific subspace for each hierarchical relation is essential and further explained in Sec. 3.3.

3.2 ConE Embedding Space and Transformations

We first introduce the embedding space that ConE operates in, and the transformations used to model hierarchical as well as non-hierarchical relations.

For ease of discussion let’s assume that the relation type is given *a priori*. In fact, knowledge about hierarchical relations (i.e., transitive closure) is explicitly available in the definition of the relation in KGs such as ConceptNet [28], WordNet [8] and Gene Ontology [9]. When such information is not available, ConE can infer “hierarchicalness” of a relation by a simple criteria with slight modification to the Krackhardt scores [29], see Appendix H.

Embedding space. The embedding space of ConE, \mathcal{S} , is a product space of d hyperbolic planes [30], resulting in a total embedding dimension of $2d$. \mathcal{S} can be denoted as $\mathcal{S} = \mathcal{B}^2 \times \mathcal{B}^2 \times \dots \times \mathcal{B}^2$. Note that this space is different from RotH embedding space [16], which is a single $2d$ -dimensional hyperbolic space. ConE’s embedding space is critical in modeling ancestor-descendant relationships for heterogeneous KGs, since it is more natural when allocating its subspaces (product space of multiple hyperbolic planes) to heterogeneous hierarchical relations.

We denote the embedding of entity $h \in \mathcal{E}$ as $\mathbf{h} = (\mathbf{h}_1, \mathbf{h}_2, \dots, \mathbf{h}_d)$ where $\mathbf{h}_i \in \mathcal{B}^2$ is the apex of the i -th 2D hyperbolic cone. We model relation r as a cone transformation on each hyperbolic plane from head entity cone to tail entity cone. Let $\mathbf{r} = (\mathbf{r}_1, \mathbf{r}_2, \dots, \mathbf{r}_d)$ be the representation of relation r . We use $\mathbf{r}_i = (s_i, \theta_i)$ to parameterize transformation for the i -th hyperbolic plane as shown in Figure 2. $s_i > 0$ is the scaling factor indicating how far to go in radial direction and $(\theta_i \cdot \phi_{\mathbf{h}_i} / \pi)$ is the rotation angle restricted by half aperture $\phi_{\mathbf{h}_i}$ ($\theta_i \in [-\pi, \pi)$). To perform hierarchical tasks such as ancestor-descendant prediction, ConE uses nested cones in each hyperbolic plane to model the partial ordering property of hierarchical relations, by the cone containment constraint in Def. 1.

Definition 1. Cone containment constraint. If entity h is an ancestor of t , then the cone embedding of t has to reside in that of the entity h , i.e., $\mathcal{C}_{t_i} \subseteq \mathcal{C}_{h_i}, \forall i \in \{1, \dots, d\}$.

The cone containment constraint can be enforced in any of the hyperbolic plane components in \mathcal{S} . Next we introduce ConE’s transformations for characterizing hierarchical and non-hierarchical patterns of relation r in triple (h, r, t) . Note that we utilize both transformations to model hierarchical relations r to capture non-hierarchical properties, i.e., symmetry, composition, etc, as well as hierarchical properties, i.e., partial ordering. We do this by performing different transformations in different subspaces of \mathcal{S} , as discussed in detail in Sec. 3.3.

Transformation for modeling non-hierarchical properties. Rotation is an expressive transformation to capture relation between entities [7]. Analogous to RotatE, we adopt **rotation transformation** f_1 to model non-hierarchical properties (Figure 3(a)). For rotation in the i -th hyperbolic plane,

$$f_1(\mathbf{h}_i, \mathbf{r}_i) = \exp_{\circ}(\mathbf{G}(\theta_i) \log_{\circ}(\mathbf{h}_i)) \quad (10)$$

where $\mathbf{G}(\theta_i)$ is the Givens rotation matrix:

$$\mathbf{G}(\theta_i) = \begin{bmatrix} \cos(\theta_i) & -\sin(\theta_i) \\ \sin(\theta_i) & \cos(\theta_i) \end{bmatrix} \quad (11)$$

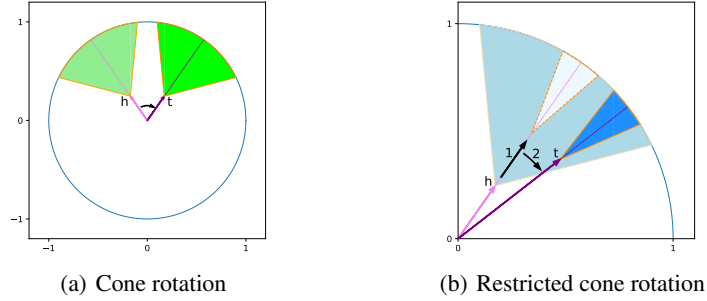


Figure 3: Transformations in ConE in Poincaré ball: (a) Cone rotation from h to t used for non-hierarchical relations; (b) Restricted rotation from the cone of parent h to the cone of child t used for hierarchical relations, where “1” corresponds to scaling and “2” to rotation (s_i, θ_i) in Eq. 12.

We also show that the rotation transformation in Eq. 10 is expressive: It can model relation patterns including symmetry, anti-symmetry, inversion, and composition (Appendix A.1).

Transformation for modeling hierarchical properties. However, f_1 cannot be directly applied to model hierarchical relations, because rotation does not obey transitive property: rotation by θ_i twice will result in a rotation of $2\theta_i$, instead of θ_i . Hence it cannot guarantee (h_1, r, h_3) when (h_1, r, h_2) and (h_2, r, h_3) are true. We use **restricted rotation transformation** f_2 to model hierarchical relations. We impose cone containment constraint to preserve partial ordering of cones after the transformation. Without loss of generality we assume relation r is a hyponym type relation, the restricted rotation from h to t in i -th hyperbolic plane is as follows (we perform restricted rotation from t to h if r is a hypernym relation):

$$f_2(\mathbf{h}_i, \mathbf{r}_i) = \exp_{\mathbf{h}_i}(s_i \cdot \mathbf{G}(\theta_i \frac{\phi_{\mathbf{h}_i}}{\pi} \bar{\mathbf{h}}_i) \bar{\mathbf{h}}_i), \mathbf{r}_i = (s_i, \theta_i) \quad (12)$$

where $\phi_{\mathbf{h}_i}$ is the half aperture of cone \mathbf{h}_i . $\bar{\mathbf{h}}_i$ is the unit vector of \mathbf{h}_i in the tangent space of \mathbf{h}_i :

$$\bar{\mathbf{h}}_i = \hat{\mathbf{h}}_i / \|\hat{\mathbf{h}}_i\|, \hat{\mathbf{h}}_i = \log_{\mathbf{h}_i} \left(\frac{1 + \|\mathbf{h}_i\|}{2\|\mathbf{h}_i\|} \mathbf{h}_i \right) \quad (13)$$

Figure 3(b) illustrates the two-step transformation described in Eq. 12, namely the scaling step and the rotation step.

3.3 ConE Model of Heterogeneous Hierarchies

In the previous section, we explained how we enforce cone containment constraint for hierarchical relations, however two challenges remain when simultaneously modeling multiple heterogeneous hierarchies: **(1) Partial ordering:** Suppose that there is a hyponym relation between entities h_1 and h_2 , and a *different* hyponym relation between entities h_2 and h_3 . Then a naïve model would enforce that the cone of h_1 contains the cone of h_2 which contains the cone of h_3 , implying that a hyponym relation exists between h_1 and h_3 , which is not correct. **(2) Expressive power:** Cone containment constraint, while ensuring hierarchical structure by geometric entailment, limits the set of possible rotation transformations and thus limits the model’s expressive power.

To address these challenges we proceed as follows. Instead of enforcing cone containment constraint in the entire embedding space, ConE proposes a novel technique to assign unique subspace for each hierarchical relation, *i.e.* we enforce cone containment constraint only in a subset of d hyperbolic planes. Next we further elaborate on this idea.

In particular, for a hierarchical relation r , we assign a corresponding subspace of \mathcal{S} , which is a product space of a subset of hyperbolic planes. Then, we use restricted rotation in the subspace and rotation in the complement space. We train ConE to enforce cone containment constraint in the relation-specific subspace. The subspace can be represented by a d -dimensional mask \mathbf{m} , $\mathbf{m}_i \in \{0, 1\}$, and $\mathbf{m}_i = 1$ indicates that cone containment is enforced in the i -th hyperbolic plane. We then extend such notation to all relations where $\mathbf{m} = \mathbf{0}$ for non-hierarchical relations.

Dataset	#entities	#relations	#training	#validation	#test	Examples of hierarchical relations
WN18RR	40,943	11	86,385	3,034	3,134	<i>hypernym, has part</i>
DDB14	9,203	14	38,233	4,000	4,000	<i>subtype of, subset of</i>
GO21	89,127	21	796,136	5,000	5,000	<i>part of, is a</i>
FB15k-237	14,541	237	272,115	17,535	20,466	<i>location/contains, /music/genre/parent_genre</i>

Table 1: Datasets statistics. Note that FB15k-237 has very few such hierarchical relations.

Our design of leveraging both transformations to model hierarchical relations is crucial in that they capture different aspects of the relation. The use of restricted rotation along with cone containment constraint serves to preserve partial ordering of a hierarchical relation in its relation-specific subspace. But restricted rotation alone is insufficient: hierarchical relations also possess other properties such as composition and symmetry that cannot be modeled by restricted rotation. Hence we augment with the rotation transformation to capture these properties, allowing composition of different hierarchical and non-hierarchical relations through rotations in the complement space. We further provide theoretical and empirical results in Appendix A to support that both transformations are of great significance to the expressiveness of our model.

Putting it all together gives us the following distance scoring function (we use $(v_i)_{i \in \{1, \dots, d\}}$ in the following to denote a d -dimensional vector \mathbf{v}):

$$\psi(h, r, t) = -\frac{1}{d}[\mathbf{m} \cdot (d_{\mathcal{B}}(f_2(\mathbf{h}_i, \mathbf{r}_i), \mathbf{t}_i))_{i \in \{1, \dots, d\}} + (\mathbf{1} - \mathbf{m}) \cdot (d_{\mathcal{B}}(f_1(\mathbf{h}_i, \mathbf{r}_i), \mathbf{t}_i))_{i \in \{1, \dots, d\}}] + b_h + b_t \quad (14)$$

where the first term corresponds to the restricted rotation in relation-specific subspace, and the second term corresponds to the rotation in complementary space. A high score indicates that cone of entity h after relation-specific transformation r is close to the cone of entity t in terms of hyperbolic distance $d_{\mathcal{B}}$. Note that b_h, b_t are the learnt radius parameters of h, t which can be interpreted as margins [15].

Subspace allocation. We assign equal dimensional subspaces for all hierarchical relations. We discuss and compare several strategies in assigning subspaces for hierarchical relations in Appendix B, including whether to use overlapping subspaces or orthogonal subspaces for different hierarchical relations, as well as the choice of dimensionality of subspaces. Overlapping subspaces (Appendix B) allow the model to perform well and enable it to scale to knowledge graphs with a large number of relations, since there are exponentially many possible overlapping subspaces that can potentially correspond to different hierarchical relations.

3.4 ConE Loss Function

We use a loss function composed of two parts. The first part of the loss function aims to ensure that for a given head entity h and relation r the distance to the true tail entity t is smaller than to the negative tail entity t' :

$$\mathcal{L}_d(h, r, t) = -\log \sigma(\psi(h, r, t)) - \sum_{t' \in \mathcal{T}} \frac{1}{|\mathcal{T}|} \log \sigma(-\psi(h, r, t')) \quad (15)$$

where (h, r, t) denotes a positive training example/triplet, and we generate negative samples (h, r, t') by substituting the tail with a random entity in $\mathcal{T} \subseteq \mathcal{E}$, a random set of entities in KG excluding t .

However, the distance loss \mathcal{L}_d does not guarantee embeddings satisfying the cone containment constraint, since the distance between transformed head embedding and tail embedding can still be non-zero after training. Hence we additionally introduce the **angle loss** (without loss of generality let r be a hyponym relation):

$$\mathcal{L}_a(h, r, t) = \mathbf{m} \cdot (\max(0, \angle_{\mathbf{h}_i} \mathbf{t}_i - \phi(\mathbf{h}_i)))_{i \in \{1, \dots, d\}} \quad (16)$$

which directly encourages cone of h to contain cone of t in relation-specific subspaces, by constraining the angle between the cones. The final loss is then a weighted sum of the distance loss and the angle loss, where weight w is a hyperparameter (We investigate the choice of w in Appendix B):

$$\mathcal{L} = \mathcal{L}_d + w \cdot \mathcal{L}_a \quad (17)$$

	WN18RR			DDB14			GO21		
	Fraction of inferred descendant pairs among all true descendant pairs in the test set								
Model	0%	50%	100%	0%	50%	100%	0%	50%	100%
Order [19]	.889	.739	.498	.731	.633	.513	.642	.592	.534
Poincaré [10]	.810	.685	.508	.976	.832	.571	.525	.519	.516
HypCone [12]	.799	.677	.504	.973	.823	.594	.554	.539	.519
RotatE [7]	.601	.593	.582	.615	.590	.565	.546	.534	.526
RotH [16]	.601	.608	.611	.609	.596	.578	.596	.583	.564
ConE	.895	.801	.679	.981	.909	.818	.789	.744	.693
Improvement (%)	+1.9%	+9.6%	+11.1%	+0.5%	+10.3%	+38.4%	+22.9%	+25.7%	+22.9%

Table 2: Ancestor-descendant prediction results in mAP (mean average precision). Best score in **bold** and second best underlined. We create different test sets that get harder as they contain more and more test cases (0%, 50%, 100%) of inferred descendant pairs.

4 Experiments

Given a KG containing many hierarchical and non-hierarchical relations, our experiments evaluate: **(A)** Performance of ConE on hierarchical reasoning task of predicting if entity h_1 is an ancestor of entity h_2 . **(B)** Performance of ConE on generic KG completion tasks.

Datasets. We use four knowledge graph benchmarks (Table 1): WordNet lexical knowledge graph (WN18RR [5, 17]), drug knowledge graph (DDB14 [18]), and a KG capturing common knowledge (FB15k-237 [31]). Furthermore, we also curated a new biomedical knowledge graph GO21, which models genes and the hierarchy of biological processes they participate in.

Model training. During training, we use Adam [32] as the optimizer and search hyperparameters including batch size, embedding dimension, learning rate, angle loss weight and dimension of subspace for each hierarchical relation. (Training details and standard deviations in Appendix G).²

We use a **single** trained model (without fine-tuning) for all evaluation tasks: On ancestor-descendant relationship prediction, our scoring function for a pair (h, t) with hierarchical relation r is the angle loss in Eq. 16 where a lower score means h is more likely to be an ancestor of t . For KG completion task we use the scoring function $\psi(h, r, t)$ in Eq. 14 to rank the triples.

4.1 Hierarchical Reasoning: Ancestor-descendant Prediction

Next we define ancestor-descendant relationship prediction task to test model’s ability on hierarchical reasoning. Given two entities, the goal makes a binary prediction if they have ancestor-descendant relationship:

Definition 2. Ancestor-descendant relationship. Entity pair (h_1, h_2) is considered to have ancestor-descendant relationship if: there exists a path from h_1 to h_2 that only contains one type of hyponym relation, or a path from h_2 to h_1 that only contains one type of hypernym relation.

Our evaluation setting is a generalization of the transitive closure prediction [19, 10, 12] which is defined only over a single hierarchy, but our knowledge graphs contain multiple hierarchies (hierarchical relations). More precisely: **(1)** When heterogeneous hierarchies coexist in the graph, we compute the transitive closure induced by each hierarchical relation separately. The test set for each hierarchical relation is a random collection sampled from all transitive closures of that relation. **(2)** To increase the difficulty of the prediction task, our evaluation also considers **inferred descendant pairs**, which are only possible to be inferred when simultaneously considering hierarchical and non-hierarchical relations in KG, due to missing links in KG. We call a descendant pair (u, v) an inferred descendant pair if their ancestor-descendant relationship can be inferred from the whole graph but *not* from the training set. For instance, $(Tree, WinePalm)$ would be an *inferred descendant pair* if the *subClass* relation between *Tree* and *PalmTree* is missing in training set. We construct the inferred descendant pairs by taking the transitive closures of the entire graph, and exclude the transitive closures of relations in the training set. In our experiments, we consider three test settings: 0%, 50%, 100%, corresponding to the fraction of inferred descendant pairs among all true descendant pairs in the test set, and the setting with a higher fraction is harder.

²The code of our paper is available at <http://snap.stanford.edu/cone>.

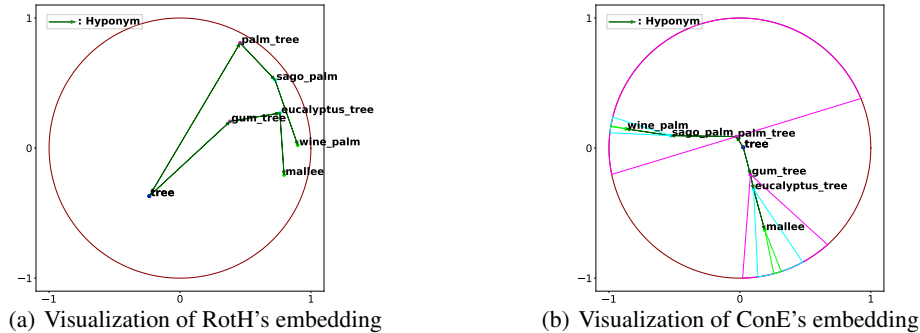


Figure 4: The embeddings of RotH and ConE, trained on WN18RR, projecting to one hyperbolic plane. We show the embedding of a family of trees, and the arrows point from higher level entities to lower level entities, representing the hierarchical relation “*Hyponym*”. Different levels of entities and their corresponding cones in ConE model (Figure 4(b)) are marked with different colors. In ConE model, the embeddings of high-level entities (e.g., tree, palm tree) are close to the center of the hyperbolic plane, while embeddings of their descendant entities (e.g., wine palm, mallee) fall in their hyperbolic cones.

On each dataset, we extract 50k ancestor-descendant pairs. For each pair, we randomly replace the true descendant with a random entity in the graph, resulting in a total of 100k pairs. Our way of selecting negative examples offsets the bias during learning that is prevalent in baseline models: the models tend to always give higher scores to pairs with a high-level node as ancestor, since high-level nodes usually have more descendants presented in training data. We replace the true descendant while keeping the true ancestor unchanged for the negative sample, and thus the model will not be able to “cheat” by taking advantage of the fore-mentioned bias. For each model, we then use its scoring function to rank all the pairs. We use the standard mean average precision (mAP) to evaluate the performance on this binary classification task. We further show the AUROC results in Appendix E.

Baselines. We compare our method with state-of-the-art methods for hierarchical reasoning, including Order embeddings [19], Poincaré embeddings [10] and Hyperbolic entailment cones [12]. Note that these methods can only handle a single hierarchical relation at a time. So each baseline trains a separate embedding for each hierarchical relation and then learns a scoring function on the embedding of the two entities. To ensure that the experiment controls the model size, we enforce that in baselines, the sum of embedding dimensions of all relations is equal to the relation embedding dimension of ConE. We also perform comprehensive hyperparameter search for all baselines (Appendix G). Although KG embedding models (RotatE [7] and RotH [16]) cannot be directly applied to this task, we adapt them to perform this task by separately training an MLP to make binary classification on ancestor-descendant pair, taking the concatenation of the two entity embeddings as input. Note that ConE outperforms these KG completion methods without even requiring additional training.

Results. Table 2 reports the ancestor-descendant prediction results of ConE and the baselines. We observe that the novel subspace transformation of ConE results in its superior performance in this task. Our model consistently outperforms baseline methods on all three datasets. As we expected, KG embedding models cannot perform well on this task (in the range of 0.5 ~ 0.6 across all settings), since they do not explicitly model the partial ordering property of the hierarchical relations. In contrast, our visualization of ConE’s embedding in Figure 4 suggests that ConE faithfully preserves the cone containment constraint in modeling hierarchical relations, while RotH’s embedding exhibit less hierarchical structure. As a result, ConE simultaneously captures the heterogeneous relation modeling and partial ordering, combining the best of both worlds. Our improvement is more significant as the fraction of inferred descendant pairs increases. This shows that ConE not only embeds a given hierarchical structure, but can also infer missing hierarchical links by modeling other non-hierarchical relations at the same time. Thanks to the restricted rotation transformation and the use of product spaces of hyperbolic planes, ConE can faithfully model the hierarchies without requiring all transitive closures in the training set. We further perform additional studies to explore reasons for the performance of each method on ancestor-descendant prediction task in Appendix E.

Lowest common ancestor prediction task. Moreover, we demonstrate flexibility and power of ConE using a hierarchical analysis task: lowest common ancestor (LCA) prediction, which requires

Model	WN18RR $\kappa = (1.00, 0.61, 0.99, 0.50)$				DDB14 $\kappa = (1.00, 0.84, 0.78, 0.18)$				GO21 $\kappa = (1.00, 0.65, 0.96, 0.22)$				FB15k-237 $\kappa = (1.00, 0.18, 0.36, 0.06)$			
	MRR	H@1	H@3	H@10	MRR	H@1	H@3	H@10	MRR	H@1	H@3	H@10	MRR	H@1	H@3	H@10
TransE [5]	.226	.017	.403	.532	.183	.103	.212	.337	.149	.066	.179	.310	.294	-	-	.465
RotatE [7]	.476	.428	.429	.571	<u>.225</u>	<u>.154</u>	<u>.245</u>	<u>.362</u>	.203	.123	<u>.234</u>	.357	.338	.241	.375	.533
TuckER [14]	.470	.443	.482	.526	.198	.137	.219	.314	<u>.205</u>	<u>.136</u>	.222	.342	.358	.266	.394	.544
HAKE [33]	<u>.496</u>	<u>.451</u>	.513	<u>.582</u>	.217	.146	.237	.361	.169	.104	.185	.295	.341	.243	.378	.535
MuRP [15]	.481	.440	.495	.566	.214	.146	.231	.349	.166	.100	.181	.301	.335	.243	.367	.518
RotH [16]	.495	.449	.514	.586	.223	.152	.245	.357	.151	.079	.171	.289	.344	.246	.380	.535
ConE	<u>.496</u>	.453	<u>.515</u>	.579	.231	.161	.252	.364	.211	.140	.237	<u>.347</u>	<u>.345</u>	<u>.247</u>	<u>.381</u>	<u>.540</u>

Table 3: Knowledge graph completion results, best out of dimension $d \in \{100, 250, 500\}$. Best score in **bold** and second best underlined. κ is a tuple denoting the 4 Krackhardt scores [29] that measure how hierarchical a graph is, higher scores mean more hierarchical. ConE achieves the best MRR and Hits@1 results in hierarchical KGs.

both the ability to model ancestor-descendant relationship and to distinguish the lowest ancestor. Results show that ConE can precisely predict LCA, outperforming over 100% on Hits@3 and Hits@10 metrics compared to previous methods (See detailed results and analysis in Appendix F).

4.2 Knowledge Graph Completion

We also experiment on knowledge graph completion task where missing links include hierarchical relations as well as non-hierarchical relations. We follow the standard evaluation setting [5].

Baselines. We compare ConE model to state-of-the-art models on knowledge graph completion task, including TransE [5], RotatE [7], TuckER [14] and HAKE [33], as well as MuRP [15] and RotH [16], which both operate on a hyperbolic space.

Results. Table 3 reports the KG completion results. Over the first three hierarchical datasets considered, ConE achieves state-of-the-art results over many recent baselines, including the recently proposed hyperbolic approaches RotH and MuRP. We also notice that the margins on Hits@1 and Hits@3 scores are much larger than Hits@10, indicating that our model provides the most accurate predictions. We further use Krackhardt scores κ to measure how hierarchical each graph is [29]. The score consists of four metrics (*connectedness*, *hierarchy*, *efficiency*, *LUBedness*), Appendix H), where if a graph is maximally hierarchical (i.e., a tree) then its Krackhardt score is (1, 1, 1, 1), and higher score on four metrics indicate a more hierarchical structure. Notice that the Krackhardt scores of FB15k-237 are approximately three times lower than those of WN18RR, DDB14 and GO21, indicating that FB15k-237 is indeed non-hierarchical. We can see that our ConE model still performs better than other hierarchical KG embedding models (RotH and MuRP) on FB15k-237 and is comparable to SOTA model (TuckER). Overall, this shows that ConE can scale to a large number of relations, and that it has competitive performance even in non-hierarchical knowledge graphs.

We further analyze the performance of ConE in low-dimensional regimes in Appendix C. Similar to previous studies, the hyperbolic-space-based ConE model performs much better than Euclidean KG embeddings in low dimensions ($d = 32$). ConE performs similar to previous hyperbolic KG embedding baselines in low dimensions, but outperforms them in high-dimensional regimes (Table 2).

Ablation study. We further compare the performance of our model with one that does not use cone restricted rotation for modeling hierarchical relations and one that does not use rotation for modeling hierarchical relations. Ablation results suggest that both transformations, i.e., cone restricted rotation and rotation, are critical in predicting missing hierarchical relations (Appendix A.2). In particular, our ablation results on each individual hierarchical relation suggest that with cone restricted rotation, ConE can simultaneously model heterogeneous hierarchical relations effectively.

5 Conclusion

In this paper, we propose ConE, a hierarchical KG embedding method that models entities as hyperbolic cones and uses different transformations between cones to simultaneously capture hierarchical and non-hierarchical relation patterns. We apply cone containment constraint to relation-specific subspaces to capture hierarchical information in heterogeneous knowledge graphs. ConE can simultaneously perform knowledge graph completion task and hierarchical task, and achieves state-of-the-art results on both tasks across three hierarchical knowledge graph datasets.

Acknowledgments and Disclosure of Funding

We gratefully acknowledge the support of DARPA under Nos. HR00112190039 (TAMI), N660011924033 (MCS); ARO under Nos. W911NF-16-1-0342 (MURI), W911NF-16-1-0171 (DURIP); NSF under Nos. OAC-1835598 (CINES), OAC-1934578 (HDR), CCF-1918940 (Expeditions), IIS-2030477 (RAPID), NIH under No. R56LM013365; Stanford Data Science Initiative, Wu Tsai Neurosciences Institute, Chan Zuckerberg Biohub, Amazon, JPMorgan Chase, Docomo, Hitachi, Intel, JD.com, KDDI, NVIDIA, Dell, Toshiba, Visa, and UnitedHealth Group. Hongyu Ren is supported by the Masason Foundation Fellowship and the Apple PhD Fellowship. Jure Leskovec is a Chan Zuckerberg Biohub investigator.

The content is solely the responsibility of the authors and does not necessarily represent the official views of the funding entities.

References

- [1] A. Hogan, E. Blomqvist, M. Cochez, C. d’Amato, G. D. Melo, C. Gutierrez, S. Kirrane, J. E. L. Gayo, R. Navigli, S. Neumaier, *et al.*, “Knowledge graphs,” *ACM Computing Surveys (CSUR)*, 2021.
- [2] Y. Hao, Y. Zhang, K. Liu, S. He, Z. Liu, H. Wu, and J. Zhao, “An end-to-end model for question answering over knowledge base with cross-attention combining global knowledge,” in *ACL*, 2017.
- [3] C. Xiong, R. Power, and J. Callan, “Explicit semantic ranking for academic search via knowledge graph embedding,” in *WWW*, 2017.
- [4] M. Zitnik, M. Agrawal, and J. Leskovec, “Modeling polypharmacy side effects with graph convolutional networks,” *Bioinformatics*, 2018.
- [5] A. Bordes, N. Usunier, A. Garcia-Duran, J. Weston, and O. Yakhnenko, “Translating embeddings for modeling multi-relational data,” in *NeurIPS*, 2013.
- [6] Y. Lin, Z. Liu, M. Sun, Y. Liu, and X. Zhu, “Learning entity and relation embeddings for knowledge graph completion,” in *AAAI*, 2015.
- [7] Z. Sun, Z.-H. Deng, J.-Y. Nie, and J. Tang, “Rotate: Knowledge graph embedding by relational rotation in complex space,” in *ICLR*, 2019.
- [8] G. A. Miller, “Wordnet: a lexical database for english,” *Communications of the ACM*, 1995.
- [9] A. Michael, A. B. Catherine, A. B. Judith, B. David, B. Heather, C. J. Michael, P. D. Allan, D. Kara, S. D. Selina, T. E. Janan, and et al, “Gene ontology: tool for the unification of biology,” *Nature genetics*, 2000.
- [10] M. Nickel and D. Kiela, “Poincaré embeddings for learning hierarchical representations,” in *NeurIPS*, 2017.
- [11] L. Vilnis, X. Li, S. Murty, and A. McCallum, “Probabilistic embedding of knowledge graphs with box lattice measures,” in *ACL*, 2018.
- [12] O.-E. Ganea, G. Bécigneul, and T. Hofmann, “Hyperbolic entailment cones for learning hierarchical embeddings,” in *ICML*, 2018.
- [13] M. Nickel and D. Kiela, “Learning continuous hierarchies in the lorentz model of hyperbolic geometry,” in *ICML*, 2018.
- [14] I. Balažević, C. Allen, and T. M. Hospedales, “Tucker: Tensor factorization for knowledge graph completion,” in *EMNLP-IJCNLP*, 2019.
- [15] I. Balazevic, C. S. Allen, and T. Hospedales, “Multi-relational poincaré graph embeddings,” in *NeurIPS*, 2019.
- [16] I. Chami, A. Wolf, D.-C. Juan, F. Sala, S. Ravi, and C. Ré, “Low-dimensional hyperbolic knowledge graph embeddings,” in *ACL*, 2020.
- [17] T. Dettmers, P. Minervini, P. Stenetorp, and S. Riedel, “Convolutional 2d knowledge graph embeddings,” in *AAAI*, 2018.
- [18] H. Wang, H. Ren, and J. Leskovec, “Entity context and relational paths for knowledge graph completion,” *arXiv preprint arXiv:2002.06757*, 2020.

- [19] I. Vendrov, R. Kiros, S. Fidler, and R. Urtasun, "Order-embeddings of images and language," in *ICLR*, 2016.
- [20] A. Lai and J. Hockenmaier, "Learning to predict denotational probabilities for modeling entailment," in *EACL*, 2017.
- [21] X. Li, L. Vilnis, D. Zhang, M. Boratko, and A. McCallum, "Smoothing the geometry of probabilistic box embeddings," in *ICLR*, 2018.
- [22] S. S. Dasgupta, M. Boratko, D. Zhang, L. Vilnis, X. L. Li, and A. McCallum, "Improving local identifiability in probabilistic box embeddings," in *NeurIPS*, 2020.
- [23] S. S. Dasgupta, X. Li, M. Boratko, D. Zhang, and A. McCallum, "Box-to-box transformation for modeling joint hierarchies," 2021.
- [24] B. Yang, W.-t. Yih, X. He, J. Gao, and L. Deng, "Embedding entities and relations for learning and inference in knowledge bases," in *ICLR*, 2015.
- [25] T. Trouillon, J. Welbl, S. Riedel, É. Gaussier, and G. Bouchard, "Complex embeddings for simple link prediction," in *ICML*, 2016.
- [26] I. Chami, Z. Ying, C. Ré, and J. Leskovec, "Hyperbolic graph convolutional neural networks," in *NeurIPS*, 2019.
- [27] O.-E. Ganea, G. Bécigneul, and T. Hofmann, "Hyperbolic neural networks," in *NeurIPS*, 2018.
- [28] R. Speer, J. Chin, and C. Havasi, "Conceptnet 5.5: An open multilingual graph of general knowledge," in *AAAI*, 2017.
- [29] D. Krackhardt, "Graph theoretical dimensions of informal organizations," *Computational organization theory*, 1994.
- [30] A. Gu, F. Sala, B. Gunel, and C. Ré, "Learning mixed-curvature representations in product spaces," in *ICLR*, 2018.
- [31] K. Toutanova and D. Chen, "Observed versus latent features for knowledge base and text inference," in *Proceedings of the 3rd workshop on continuous vector space models and their compositionality*, 2015.
- [32] D. P. Kingma and J. Ba, "Adam: A method for stochastic optimization," in *ICLR*, 2015.
- [33] Z. Zhang, J. Cai, Y. Zhang, and J. Wang, "Learning hierarchy-aware knowledge graph embeddings for link prediction," in *AAAI*, 2020.
- [34] J. Piñero, J. M. Ramírez-Anguita, J. Saüch-Pitarch, F. Ronzano, E. Centeno, F. Sanz, and L. I. Furlong, "The DisGeNET knowledge platform for disease genomics: 2019 update," *Nucleic Acids Research*, 2019.
- [35] A. P. Davis, C. J. Grondin, R. J. Johnson, D. Sciaky, J. Wiegiers, T. C. Wiegiers, and C. J. Mattingly, "Comparative toxicogenomics database (ctd): update 2021," *Nucleic acids research*, 2021.
- [36] O. Bodenreider, "The Unified Medical Language System (UMLS): integrating biomedical terminology," *Nucleic Acids Research*, 2004.
- [37] D. S. Wishart, C. Knox, A. C. Guo, D. Cheng, S. Shrivastava, D. Tzur, B. Gautam, and M. Hassanali, "DrugBank: a knowledgebase for drugs, drug actions and drug targets," *Nucleic Acids Research*, 2007.
- [38] Y. D. Feunang, R. Eisner, C. Knox, L. Chepelev, J. Hastings, G. Owen, E. Fahy, C. Steinbeck, S. Subramanian, E. Bolton, *et al.*, "Classyfire: automated chemical classification with a comprehensive, computable taxonomy," *Journal of cheminformatics*, 2016.
- [39] E. L. Carolyn, "Medical subject headings (mesh)," *Bulletin of the Medical Library Association*, 2000.
- [40] C. Ruiz, M. Zitnik, and J. Leskovec, "Discovery of disease treatment mechanisms through the multiscale interactome," *bioRxiv*, 2020.

A Theoretical and empirical evidence for ConE's design choice

Here we provide theoretical and empirical results to support that ConE's design choice makes sense, i.e., both rotation transformation and restricted transformation play a crucial role to the expressiveness of the model.

A.1 Proof for transformations

A.1.1 Proof for rotation transformation

We will show that the rotation transformation in Eq. 10 can model all relation patterns that can be modeled by its Euclidean counterpart RotatE [7].

Three most common relation patterns are discussed in [7], including symmetry pattern, inverse pattern and composition pattern. Let \mathbb{T} denote the set of all true triples. We formally define the three relation patterns as follows.

Definition 3. *If a relation r satisfies symmetric pattern, then*

$$\forall h, t \in \mathcal{E}, (h, r, t) \in \mathbb{T} \Rightarrow (t, r, h) \in \mathbb{T}$$

Definition 4. *If relation r_1 and r_2 satisfies inverse pattern, i.e., r_1 is inverse to r_2 , we have*

$$\forall h, t \in \mathcal{E}, (h, r_1, t) \in \mathbb{T} \Rightarrow (t, r_2, h) \in \mathbb{T}$$

Definition 5. *If relation r_1 is composed of r_2 and r_3 , then they satisfies composition pattern,*

$$\forall h, m, t \in \mathcal{E}, (h, r_2, m) \in \mathbb{T} \wedge (m, r_3, t) \in \mathbb{T} \Rightarrow (h, r_1, t) \in \mathbb{T}$$

Theorem 1. *Rotation transformation can model symmetric pattern.*

Proof. If r is a symmetric relation, then for each triple (h, r, t) , its symmetric triple (t, r, h) is also true. For $i \in \{1, 2, \dots, d\}$, we have

$$\mathbf{t}_i = \exp_{\mathbf{o}}(\mathbf{G}(\theta_i) \log_{\mathbf{o}}(\mathbf{h}_i)), \mathbf{h}_i = \exp_{\mathbf{o}}(\mathbf{G}(\theta_i) \log_{\mathbf{o}}(\mathbf{t}_i))$$

Let \mathbf{I} denote the identity matrix. By taking logarithmic map on both sides, we have

$$\log_{\mathbf{o}}(\mathbf{t}_i) = \mathbf{G}(\theta_i) \log_{\mathbf{o}}(\mathbf{h}_i), \log_{\mathbf{o}}(\mathbf{h}_i) = \mathbf{G}(\theta_i) \log_{\mathbf{o}}(\mathbf{t}_i) \Rightarrow \mathbf{G}^2(\theta_i) = \mathbf{I}$$

which holds true when $\theta_i = -\pi$ or $\theta_i = 0$ (still we assume $\theta_i \in [-\pi, \pi)$).

Theorem 2. *Rotation transformation can model inverse pattern.*

Proof. If r_1 and r_2 are inverse relations, then for each triple (h, r_1, t) , its inverse triple (t, r_2, h) also holds. Let $(\theta_i)_{i \in \{1, \dots, d\}}$ denote the rotation parameter of relation r_1 and $(\alpha_i)_{i \in \{1, \dots, d\}}$ denote the rotation parameter of relation r_2 . Similar to the proof of Theorem 1, we take logarithmic map on rotation transformation, then

$$\log_{\mathbf{o}}(\mathbf{t}_i) = \mathbf{G}(\theta_i) \log_{\mathbf{o}}(\mathbf{h}_i), \log_{\mathbf{o}}(\mathbf{h}_i) = \mathbf{G}(\alpha_i) \log_{\mathbf{o}}(\mathbf{t}_i) \Rightarrow \mathbf{G}(\theta_i) \mathbf{G}(\alpha_i) = \mathbf{I}$$

which holds true when $\theta_i + \alpha_i = 0$.

Theorem 3. *Rotation transformation can model composition pattern.*

Proof. If relation r_1 is composed of r_2 and r_3 , then triple (h, r_1, t) exists when (h, r_2, m) and (m, r_3, t) exist. Let $(\theta_i)_{i \in \{1, \dots, d\}}$, $(\alpha_i)_{i \in \{1, \dots, d\}}$, $(\beta_i)_{i \in \{1, \dots, d\}}$, denote their rotation parameters correspondingly. Still we take logarithmic map on rotation transformation and it can be derived that

$$\begin{aligned} \log_{\mathbf{o}}(\mathbf{t}_i) &= \mathbf{G}(\theta_i) \log_{\mathbf{o}}(\mathbf{h}_i), \log_{\mathbf{o}}(\mathbf{m}_i) = \mathbf{G}(\alpha_i) \log_{\mathbf{o}}(\mathbf{h}_i), \\ \log_{\mathbf{o}}(\mathbf{t}_i) &= \mathbf{G}(\beta_i) \log_{\mathbf{o}}(\mathbf{m}_i) \Rightarrow \mathbf{G}(\theta_i) = \mathbf{G}(\alpha_i) \mathbf{G}(\beta_i) \end{aligned}$$

which holds true when $\theta_i = \alpha_i + \beta_i$ or $\theta_i = \alpha_i + \beta_i + 2\pi$ or $\theta_i = \alpha_i + \beta_i - 2\pi$.

Model	All relations			Hierarchical relations			Non-hierarchical relations		
	MRR	H@1	H@10	MRR	H@1	H@10	MRR	H@1	H@10
RotC	.481	.444	.551	.209	.157	.312	.936	.923	.951
ConE	.496	.453	.579	.231	.171	.355	.939	.930	.952
Improvement (%)	+3.1%	+2.0%	+5.1%	+10.5%	+8.9%	+13.8%	+0.3%	+0.7%	+0.1%

Table 4: Results of ablation study on restricted rotation, for knowledge graph completion task on WN18RR. Results in three columns are conducted on all relations during evaluation, only hierarchical relations during evaluation and only non-hierarchical relations during evaluation.

Relation	RotC	ConE	Improvement
<i>hypernym</i>	.175	.193	+10.3%
<i>instance hypernym</i>	.373	.406	+8.8%
<i>member meronym</i>	.230	.231	+0.4%
<i>synset domain topic of</i>	.382	.413	+8.1%
<i>has part</i>	.208	.213	+2.4%
<i>member of domain usage</i>	.200	.345	+72.5%
<i>member of domain region</i>	.142	.244	+71.8%

Table 5: Comparison of MRR for all hierarchical relations in WN18RR between RotC and ConE.

A.1.2 Proof for restricted rotation transformation

Theorem 4. *Restricted rotation transformation always satisfies the cone containment constraint.*

Proof. For any triple (h, r, t) where r is a hierarchical relation, we will prove that cone containment constraint is satisfied after the restricted rotation from h to t , i.e., $\mathcal{C}_{f_2(\mathbf{h}_i, \mathbf{r}_i)} \subseteq \mathcal{C}_{\mathbf{h}_i}$. By the transitivity of entailment cone as in Eq. 6, we only need to prove $f_2(\mathbf{h}_i, \mathbf{r}_i) \in \mathcal{C}_{\mathbf{h}_i}$, which is

$$\angle_{\mathbf{h}_i} f_2(\mathbf{h}_i, \mathbf{r}_i) \leq \phi_{\mathbf{h}_i} \quad (18)$$

according to the cone expression in Eq. 8. We can calculate the angle, denoted as φ , on the left hand side of the equation in tangent space $\mathcal{T}_{\mathbf{h}_i} \mathcal{B}$ (which is equipped with Euclidean metric),

$$\begin{aligned} \varphi &= \angle_{\mathbf{h}_i} f_2(\mathbf{h}_i, \mathbf{r}_i) \\ &= \angle(\log_{\mathbf{h}_i}(\frac{1 + \|\mathbf{h}_i\|}{2\|\mathbf{h}_i\|} \mathbf{h}_i), \log_{\mathbf{h}_i} f_2(\mathbf{h}_i, \mathbf{r}_i)) \\ &= \angle(\bar{\mathbf{h}}_i, \mathbf{G}(\theta_i \frac{\phi_{\mathbf{h}_i}}{\pi} \bar{\mathbf{h}}_i)) = |\theta_i \frac{\phi_{\mathbf{h}_i}}{\pi}| \end{aligned} \quad (19)$$

For $\theta_i \in [-\pi, \pi)$, we have $|\theta_i \frac{\phi_{\mathbf{h}_i}}{\pi}| \leq \phi_{\mathbf{h}_i}$. Therefore Eq. 18 holds, suggesting that cone containment constraint is satisfied.

A.2 Ablation studies on transformations in ConE

Empirically, we show that our design of transformations in ConE is effective: both restricted rotation transformation in the relation-specific subspace and the rotation transformation in the complement space are indispensable to the performance of our model on knowledge graph completion task.

A.2.1 Ablation study on restricted rotation transformation

Restricted rotation transformation is vital in enforcing cone containment constraint, and thus it is indispensable to ConE’s performance on hierarchical tasks. However, its effect on knowledge graph completion task remains unknown. We further compare the performance of ConE with one that does not use cone restricted rotation for modeling hierarchical relations, which we name as RotC. Specifically, RotC is the same as ConE, except that it applies rotation transformation to all relations, and the cone angle loss as in Eq. 16 is excluded.

Results. Ablation results are shown in Table 4. We can see remarkable improvement on knowledge graph completion task after applying restricted rotation transformation to hierarchical relations,

Model	MRR	H@1	H@3	H@10
ConE w/o rotation	.397	.329	.433	.526
ConE	.496	.453	.515	.579

Table 6: Results of ablation study on rotation, for knowledge graph completion task on WN18RR. ConE w/o rotation is the model that applies restricted rotation in the whole embedding space for hierarchical relations.

(a) On knowledge graph completion					(b) On ancestor-descendant completion, in mAP metric			
Model	MRR	H@1	H@3	H@10	Model	0%	50%	100%
Orthogonal	.493	.449	.512	.577	Orthogonal	.930	.863	.772
Overlapping	.495	.451	.513	.582	Overlapping	.928	.862	.773

Table 7: Comparison between orthogonal subspaces and overlapping subspaces on WN18RR benchmark.

especially in predicting missing hierarchical relations. The results suggest that restricted rotation transformation helps model hierarchical relation patterns.

Individual results for each hierarchical relation. To further demonstrate that ConE can deal with multiple hierarchical relations simultaneously with our proposed restricted rotation in subspaces, we report the improvement for knowledge graph completion on each type of missing hierarchical relation after adding cone restricted rotation, shown in Table 5. We observe significant improvement on *all* hierarchical relations, which shows our way of modeling heterogeneous hierarchies to be effective. Note that up to 72% improvement is achieved for some hierarchical relation thanks to the restricted rotation operation in ConE.

A.2.2 Ablation study on rotation transformation

To address the importance of rotation transformation in modeling hierarchical relations, we present the performance comparison between ConE that uses rotation and one that does not use rotation for hierarchical relations on WN18RR. The results in Table 6 suggest that rotation transformation for hierarchical relations is significant to the model’s expressive power.

B Strategies in assigning relation-specific subspace and embedding space curvature

We compare several strategies for assigning subspace for each hierarchical relation. For simplicity, we assign equal dimension subspaces for all hierarchical relations.

B.1 Overlapping subspaces and orthogonal subspaces

First, we compare the results on ancestor-descendant prediction and knowledge graph completion between different subspace assigning strategies, i.e., using overlapping subspaces and using orthogonal subspaces. We conduct the experiment on WN18RR dataset. For both strategies, the embedding dimension $d = 500$ and the subspace dimension $d_s = 70$ for each hierarchical relation (7 hierarchical relations in total hence it is possible to assign orthogonal subspaces). For assigning overlapping subspaces, since it is impossible to investigate all possible combinations, we randomly choose d_s out of d number of hyperbolic planes to each hierarchical relation. To avoid the randomness of the results due to our method in assigning overlapping subspaces, we repeat the experiment multiple times and take the average for the final result.

Results. Table 7 reports the results on ancestor-descendant prediction task as well as knowledge graph completion task. Between two strategies, ConE performs slightly better on knowledge graph completion task under overlapping subspaces, while their performances are comparable on ancestor-descendant prediction task. The most significant advantage for using overlapping subspaces is that it does not suffer from limitation of subspace dimension, while for orthogonal subspaces the subspace dimension can be at most d/n where n is the number of hierarchical relations.

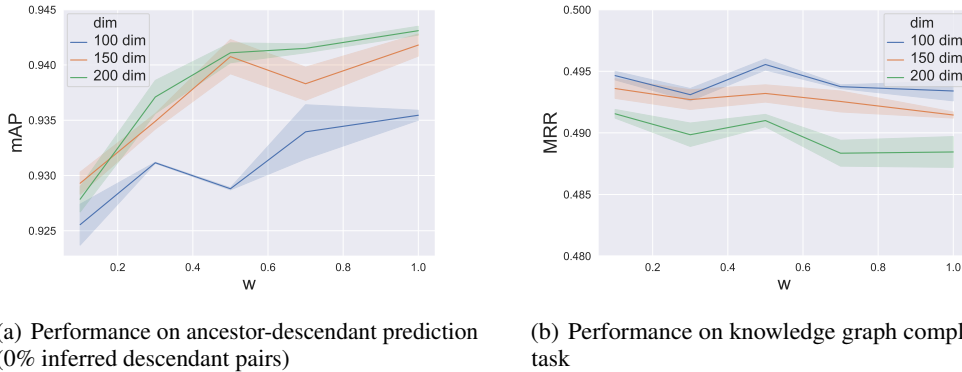


Figure 5: Performance of two tasks on WN18RR under varying strategies, including angle loss weight $w \in \{0.1, 0.3, 0.5, 0.7, 1.0\}$, dimension of subspace $d_s \in \{100, 150, 200\}$. Due to larger number of dimensions used per subspace, we use overlapping subspace strategy to assign relation-specific subspaces.

Model	MRR	H@1	H@3	H@10
RotatE	.387	.330	.417	.491
MuRP	.465	.420	.484	<u>.544</u>
RotH	.472	<u>.428</u>	.490	.553
ConE	<u>.471</u>	.436	<u>.486</u>	.537

Table 8: Knowledge graph completion results for low-dimensional embeddings ($d = 32$) on WN18RR. Best score in **bold** and second best underlined.

B.2 Subspace dimension and angle loss weight

We also study the effect of subspace dimension d_s and angle loss weight w (in Eq. 17) on the performance of ConE. We use overlapping subspaces where we randomly choose d_s out of $d = 500$ hyperbolic planes to compose the subspace for each hierarchical relation.

Results. Figure 5 reports the results on both tasks in curves. We notice a trade-off between two tasks for subspace dimension, where a larger dimension contributes to better performance on hierarchical task, while limiting the performance on knowledge graph completion task. With larger angle loss weight w , cone containment constraint is enforced more strictly, and thus the performance of ConE on hierarchical task improves as shown in Figure 5(a). On the other hand, ConE reaches peak performance on knowledge graph completion task at $w = 0.5$.

B.3 Space curvature

Aside from setting fixed curvature $c = -1$, we also investigate on learning curvature, as [16] suggests that fixing the curvature has a negative impact on performance of RotH. With learning curvature, ConE has (MRR, H@1, H@3, H@10) = (0.485, 0.441, 0.501, 0.570), on WN18RR benchmark, lower than original ConE with fixed curvature with (MRR, H@1, H@3, H@10) = (0.496, 0.453, 0.515, 0.579). The reason why RotH [16] needs learning space curvature while ConE does not lie in the choice of embedding space: RotH uses a $2d$ -dimensional hyperbolic space while ConE uses product space of d hyperbolic planes. Our embedding space is less sensitive to its curvature, since for every subspace, the hierarchical structure for the corresponding single relation is less complex (than the entire hierarchy), and can thus be robust to choices of curvatures.

C Knowledge graph completion results in low dimensions

One of the main benefits of learning embeddings in hyperbolic space is that it can model well even in low embedding dimensionalities. We report in Table 8 the performance of ConE in the

Model	Percentage of inferred descendant pairs								
	WN18RR			DDB14			GO21		
	0%	50%	100%	0%	50%	100%	0%	50%	100%
Order	.859	.676	.495	.971	.745	.533	.643	.587	.542
Poincaré	.784	.649	.511	.981	.763	.541	.534	.529	.526
HypCone	.767	.635	.501	.976	<u>.773</u>	<u>.560</u>	.553	.541	.531
RotatE	.599	.601	<u>.599</u>	.506	.505	.514	.622	.607	<u>.598</u>
RotH	.559	.567	<u>.574</u>	.525	.519	.517	.630	<u>.612</u>	.594
ConE	.874	.762	.657	<u>.979</u>	.888	.802	.704	.653	.601
Improvement (%)	+1.7%	+12.7%	+9.7%	-0.2%	+14.9%	+43.2%	+9.5%	+6.7%	+0.5%

Table 9: Ancestor-descendant prediction results in AUROC. Best score in **bold** and second best underlined.

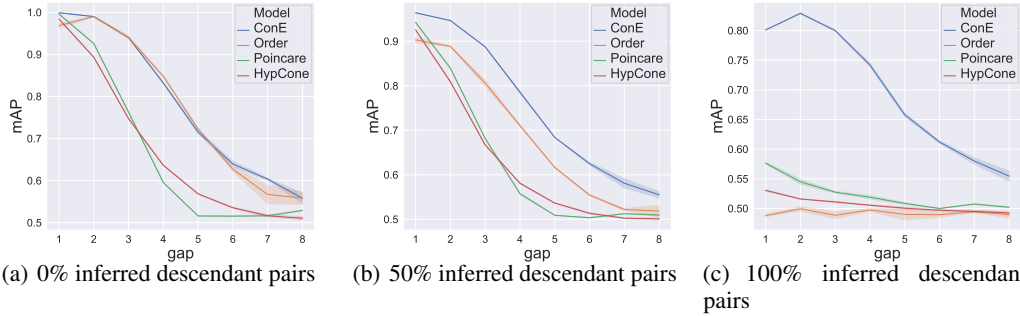


Figure 6: mAP results on ancestor-descendant prediction under different hierarchy gaps (Def. 6) on WN18RR.

low-dimensional setting for $d = 32$ on WN18RR dataset. Our performance is comparable to other hyperbolic embedding models (MuRP and RotH), while being superior to Euclidean embedding models (RotatE).

D Dataset details and GO21 dataset

WN18RR is a subset of WordNet [8], which features lexical relationships between word senses. More than 60% of all triples characterize hierarchical relationships. DDB14 is collected from Disease Database, which contains terminologies including diseases, drugs, and their relationships. Among all triples in DDB14, 30% include hierarchical relations.

GO21 is a biological knowledge graph containing genes, proteins, drugs and diseases as entities, created based on several widely used biological databases, including Gene Ontology [9], Disgenet [34], CTD [35], UMLS [36], DrugBank [37], ClassyFire [38], MeSH [39] and PPI [40]. It contains 80k triples, while nearly 35% of which include hierarchical relations. The dataset will be made public at publication.

E AUROC results and hierarchy gap studies on ancestor-descendant prediction

We show in Table 9 the results with AUROC (Area Under the Receiver Operating Characteristic curve) metric on ancestor-prediction tasks. It can be seen that the performance trend with AUROC metric is similar to that in Table 2 with mAP metric.

Definition 6. Hierarchy gap. The hierarchy gap of an ancestor-descendant pair (u, v) is the length of path consisting of the same hierarchical relation connecting u and v .

Moreover, we evaluate the classification performance of our model against other baselines over ancestor-descendant pairs with different hierarchy gaps (Def. 6), as shown in Figure 6. The trend of the curves is in line with our expectation: performance gets worse with larger hierarchy gaps.

Model	1-Hop			2-Hop			3-Hop		
	H@1	H@3	H@10	H@1	H@3	H@10	H@1	H@3	H@10
Order [19]	39.2%	55.1%	61.6%	27.6%	40.1%	<u>54.7%</u>	15.1%	24.7%	42.2%
Poincaré [10]	1.5%	3.0%	8.0%	<u>31.4%</u>	34.6%	38.5%	<u>19.5%</u>	23.1%	38.5%
HypCone [12]	15.0%	30.7%	53.0%	16.5%	30.1%	43.3%	12.4%	<u>38.1%</u>	<u>52.0%</u>
RotatE [7]	54.7%	63.3%	69.7%	20.4%	29.0%	35.8%	14.6%	18.3%	20.7%
RotH [16]	<u>79.7%</u>	<u>86.0%</u>	<u>86.4%</u>	29.1%	35.7%	40.2%	13.9%	18.0%	21.9%
ConE	98.1%	99.3%	99.4%	48.6%	89.6%	97.3%	24.2%	55.6%	80.6%

Table 10: LCA prediction task results on the WN18RR dataset. N-hop means that for any pair (u, v) in the test set, the true LCA w has hierarchy gaps (Def. 6) at most N to u and v . The task difficulty increases as the maximum number of hops to ancestor increases. Best score in **bold** and second best underlined.

Under the setting of 0% inferred pairs, the performance of Poincaré embedding and Hyperbolic cone embedding drops dramatically as hierarchy gap increases, suggesting that transitivity is not well-preserved in these embeddings under heterogeneous setting. In all settings (0%, 50% and 100% inferred descendant pairs), ConE significantly outperforms baselines.

F Hierarchical analysis: LCA prediction

We further demonstrate flexibility and power of ConE using a new hierarchical task, lowest common ancestor (LCA) prediction. Given two entities, we want to find the most distinguishable feature they have in common, e.g., $LCA(WinePalm, SugarPalm)=PalmTree$ in Figure 1(a). Formally, let l_{uv} denote the hierarchy gap (Def. 6) between u and v and $l_{uv} = \infty$ if u is not an ancestor of v , then we define $LCA(u, v) = \operatorname{argmin}_{w \in \mathcal{E}} [l_{wu} + l_{wv}]$. Note that if multiple common ancestors have the same sum of hierarchy gap, we consider any of them to be correct. ConE uses ranking over all entities to predict LCA, with the following scoring function for w to be the LCA of u and v :

$$\Phi_w(u, v) = \mathbf{m} \cdot (2\phi(\mathbf{w}_i) - \angle_{\mathbf{w}_i} \mathbf{u}_i - \angle_{\mathbf{w}_i} \mathbf{v}_i)_{i \in \{1, \dots, d\}} \quad (20)$$

We evaluate the LCA prediction task on WN18RR dataset, and use the embeddings of our trained ConE model to rank and make prediction. Standard evaluation metrics including Hits at N (Hits@N) are calculated. Since no previous KG embedding method can directly perform the LCA task, we adapt them by training an MLP layer with the concatenation of the two entity embeddings as input and output the predicted entity (trained as a multi-label classification task).

Results. Table 10 reports the LCA prediction results. ConE can provide much more precise LCA prediction than baseline methods, and the performance gap increases as the number of hops to ancestor increases. We summarize the reasons that ConE performs superior to previous methods on LCA prediction: the task requires (1) the modeling of partial ordering for ancestor-descendant relation prediction and (2) an expressive embedding space for distinguishing the lowest ancestor. Only our ConE model is able to do both.

G Training details

We report the best hyperparameters of ConE on each dataset in Table 11. As suggested in [12], hyperbolic cone is hard to optimize with randomized initialization, so we utilize RotC model (which only involves rotation transformation) as pretraining for ConE model, and recover the entity embedding from the pretrained RotC model with 0.5 factor. For both the pretraining RotC model and ConE model, we use Adam [32] as the optimizer. Self-adversarial training has been proven to be effective in [7], we also use self-adversarial technique during training for ConE with self-adversarial temperature $\alpha = 0.5$.

Knowledge graph completion. Standard evaluation metrics including Mean Reciprocal Rank (MRR), Hits at N (H@N) are calculated in the filtered setting where all true triples are filtered out during ranking.

In our experiments, we train and evaluate our model on a single GeForce RTX 3090 GPU. We train the model for 500 epochs, 1000 epochs, 100 epochs and 600 epochs on WN18RR, DDB14, GO21

Dataset	embedding dim	learning rate	batch size	negative samples	subspace dim	angle loss weight
WN18RR	500	0.001	1024	50	100	0.5
DDB14	500	0.001	1024	50	50	0.7
GO21	500	0.005	1024	50	50	0.1
FB15k-237	500	0.0001	1024	100	-	-

Table 11: Best hyperparameter setting of ConE on four datasets.

and FB15k-237 respectively, and the training procedure takes 4hrs, 2hrs, 6hrs, 6hrs on these four datasets. On knowledge graph completion task, ConE model has standard deviation less than 0.001 on MRR metric across all datasets. On ancestor-descendant classification task, ConE model has standard deviation less than 0.01 on mAP metric across all datasets.

For all baselines mentioned in our work, we also perform comprehensive hyperparameter search. Specifically, for KG embedding methods (TransE [5], RotatE [7], TuckER [14], HAKE [33], MuRP [15], RotH [16]), we search for embedding dimension in $\{100, 250, 500\}$, batch size in $\{256, 512, 1024\}$, learning rate in $\{0.01, 0.001, 0.0001\}$ and negative sampling size in $\{50, 100, 250\}$. For partial order modeling methods (Order [19], Poincaré [10], HypCone [12]), we search for embedding dimension in $\{50, 100, 250, 500\}$ and learning rate in $\{0.001, 0.0001, 0.00001\}$.

H Krackhardt hierarchical measurement

H.1 Krackhardt score for the whole graph

The paper [29] proposes a set of scores to measure how hierarchical a graph is. It includes four scores: (*connectedness*, *hierarchy*, *efficiency*, *LUBedness*). Each score range from 0 to 1, and higher scores mean more hierarchical. When all four scores equal to 1, the digraph is a tree, normally considered as the most hierarchical structure. We make some adjustments to the computation of the metrics from the original paper to adapt them to heterogeneous graphs.

1. *Connectedness*. Connectedness measures the connectivity of a graph, where a connected digraph (each node can reach every other node in the underlying graph) will be given score 1 and the score goes down with more disconnected pairs. Formally, the degree of connectedness is

$$connectedness = \frac{c}{n(n-1)/2} \quad (21)$$

where c is the number of connected pairs and n is the total number of nodes.

2. *Hierarchy*. Hierarchy measures the order property of the relations in the graph. If for each pair of nodes such that one node u can reach the other node v , v cannot reach u , then the hierarchy score is 1. In knowledge graph this implies that if $(u, rel, v) \in \mathbb{T}$ then $(v, rel, u) \notin \mathbb{T}$. Let T denote the set of ordered pairs (u, v) such that u can reach v , and $S = \{(v, u) | (u, v) \in T, v \text{ cannot reach } u\}$, the degree of hierarchy is defined as

$$hierarchy = \frac{|S|}{|T|} \quad (22)$$

3. *Efficiency*. Another condition to make sure that a structure is a tree is that the graph contains exactly $n - 1$ edges, given n number of nodes. In other word, the graph cannot have redundant edges. The degree of efficiency is defined as

$$efficiency = 1 - \alpha \cdot \frac{m - (n - 1)}{(n - 1)(n - 2)/2} \quad (23)$$

where m is the number of edges in the graph. Numerator $m - (n - 1)$ is the number of redundant edges in the graph while denominator $(n - 1)(n - 2)/2$ is the maximum number of redundant edges possible. In the original paper [29], α is set to 1, in our case we take $\alpha = 500$ to make the gap larger since common knowledge graph are always sparse.

4. *LUBedness*. The last condition for a tree structure is that every pair of nodes has a least upper bound, which is the same as our defined LCA concept (in Sec. F) in knowledge graph case. Different from the homogeneous setting in [29], we still restrict LCA to a single relation (same relation on the

paths between the pair of nodes and their LCA), since heterogeneous hierarchies may exist in a single KG. Let $T = \{(u, v) | (u, v) \text{ has a LCA}\}$, then the degree of LUBedness is defined as

$$LUBedness = \frac{|T|}{n(n-1)} \quad (24)$$

H.2 Hierarchical-ness scores for each relation

Here we introduce the Hierarchical-ness scores for each relation, which is a modified version of original Krackhardt scores on the induced subgraph of a relation. We observe, using the groundtruth hypernym, hyponym and non-hierarchical relations in existing datasets (WN18RR, DDB14, GO21), that the Hierarchical-ness scores for hypernym, hyponym and non-hierarchical relations can be easily separated via decision boundaries. To apply ConE on a dataset where the type of relation is not available, we can compute the Hierarchical-ness scores of the relations, and classify the hierarchical-ness of the relations via the decision boundaries.

Here we introduce the computation of our Hierarchical-ness scores, which contain two terms: (*asymmetry*, *tree_likeness*).

1. *Asymmetry*. The *asymmetry* metric is the same as *hierarchy* metric in Krackhardt scores.

2. *Tree_likeness*. The *tree_likeness* metric is adapted from the *LUBedness* metric in Krackhardt scores where three adjustments are made:

(a) The subgraph induced by a single relation is not guaranteed to be connected, and forest is a typical hierarchical structure in such a disconnected graph. We cannot make sure every pair of nodes are in the same tree, and thus we evaluate on all connected pairs and check whether they have an LCA. Let P denote the set of pairs (u, v) such that u and v are connected, and the set $Q = \{(u, v) | (u, v) \in P \text{ and } (u, v) \text{ has a LCA}\}$. Then our new *LUBedness'* for disconnected graph is calculated as

$$LUBedness' = \frac{|Q|}{|P|} \quad (25)$$

(b) We want to distinguish true hierarchical relations from common 1-N relations, where the transitivity property may not hold (for example, *participants* of some event entity is a 1-N relation, yet it does not define a partial ordering since the head entity and tail entity are not the same type of entities). This kind of relation can be characterized by 1-depth trees in their induced subgraph, while hierarchical relations usually induce trees of greater depth. Hence we add punishment to the induced subgraphs containing mostly 1-depth trees to exclude non-hierarchical 1-N relations. In particular, let E denote the set of edges, and $S = \{u | \exists v : (u, v) \in E \text{ or } (v, u) \in E\}$, $T = \{u | \exists v : (u, v) \in E \text{ and } (v, u) \in E\}$. If 1-depth trees are prevalent in the structure, then $|T|$ is approximately 0. We define the punishment decaying factor (lower means more punishment):

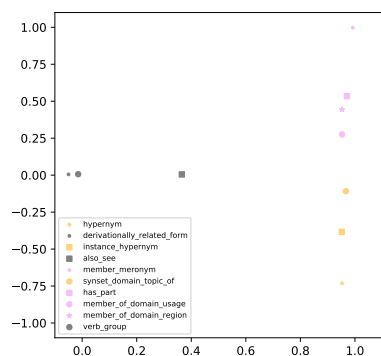
$$d = \frac{|T|}{|S|} \quad (26)$$

(c) *LUBedness* metric also depends on the direction of the relation, since LCA exists only if the relations are hyponym type (pointing from parent node to child nodes) while hypernym type relation can also define a partial ordering and considered as hierarchical relation. Hence for each relation, we define two induced graphs G and G_{rev} , G in original direction and G_{rev} in reversed direction. We calculate the *LUBedness* metric of the two graphs, if the score of G is much higher than the score of G_{rev} then the relation is of hyponym type, and vice versa. We take the absolute value of $LUBedness'(G) - LUBedness'(G_{rev})$ as the score to measure the hierarchical-ness while its sign to check if it is of hypernym type or hyponym type.

Finally, our *tree_likeness* metric is calculated through

$$tree_likeness = (LUBedness'(G) - LUBedness'(G_{rev})) / \max(1, (\log_{10}(d))^2) \quad (27)$$

We show that our Hierarchical-ness scores indicate the type of relation on WN18RR, DDB14 and GO21 datasets. In Figure 7(a), Figure 8(a), Figure 9(a), we visualize the two-dimensional scores for each relation in the three datasets. Groundtruth hypernym type relations are colored in orange and hyponym relations are colored in violet. We can see that hypernym type relations are clustered

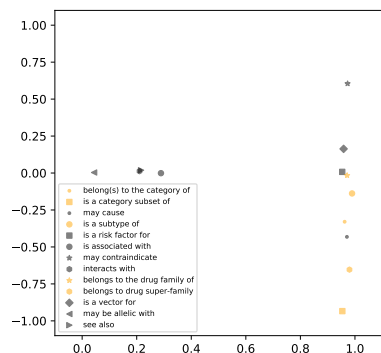


(a) Hierarchical-ness score visualization for all relations.

Relation	Score	Hierarchical
<i>hypernym</i>	2.0	true
<i>member meronym</i>	2.0	true
<i>has part</i>	2.0	true
<i>member of domain region</i>	1.9	true
<i>instance hypernym</i>	1.7	true
<i>member of domain usage</i>	1.5	true
<i>synset domain topic of</i>	1.2	true
<i>also see</i>	0.4	false
<i>derivationally related form</i>	0.0	false
<i>verb group</i>	0.0	false
<i>similar to</i>	0.0	false

(b) Relation type classification based on Hierarchical-ness score.

Figure 7: Results on WN18RR dataset. (a) Score (*asymmetry*, *tree_likeness*) as (x, y) coordinate in visualization. Orange dots denote hypernym type relations, violet dots denote hyponym type relations and black dots denote non-hierarchical relations. (b) Relations above the line are predicted to be hierarchical relations, and ground-truth relation type are in the third column. All relations are correctly predicted.



(a) Hierarchical-ness score visualization for all relations.

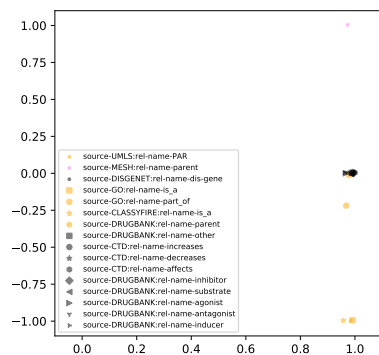
Relation	Score	Hierarchical
<i>is a category subset of</i>	2.0	true
<i>belongs to drug super-family</i>	2.0	true
<i>has part</i>	2.0	true
<i>may contraindicate</i>	1.9	false*
<i>may cause</i>	1.8	false*
<i>belong(s) to the category of</i>	1.7	true
<i>belong(s) to the category of</i>	1.2	true
<i>is a vector for</i>	1.3	false*
<i>is a subtype of</i>	1.3	true
<i>belongs to the drug family of</i>	1.1	true
<i>is a risk factor for</i>	1.0	false
<i>see also</i>	0.3	false
<i>interacts with</i>	0.3	false
<i>may be allelic with</i>	0.1	false
<i>is an ingredient of</i>	0.0	false

(b) Relation type classification based on Hierarchical-ness score.

Figure 8: Results on DDB14 dataset. (a) Score (*asymmetry*, *tree_likeness*) as (x, y) coordinate in visualization. Orange dots denote hypernym type relations, violet dots denote hyponym type relations and black dots denote non-hierarchical relations. (b) Relations above the line are predicted to be hierarchical relations, and ground-truth relation type are in the third column. Predictions are correct except three non-hierarchical relations are inferred to be hierarchical relations, while these relations do have soft-hierarchical property.

in lower right while hyponym type relations are clustered in upper right, indicating that hypernym type relations have large *asymmetry* score and large positive *tree_likeness* score while hyponym type relations have large *asymmetry* score and large negative *tree_likeness* score. Moreover, We use $asymmetry + |tree_likeness|$ as the total Hierarchical-ness score and set threshold 1.1 to separate hierarchical relations and non-hierarchical relations. As shown in Figure 7(b), Figure 8(b), Figure 9(b), our classification results highly conform to the groundtruth relation type.

Additionally, we use our Hierarchical-ness scores to distinguish hierarchical relations from 237 relations in FB15k-237, as shown in Figure 10(a), Figure 10(b). Since there is no labeling of relation type in FB15k-237, we do not have groundtruth. We label the relations that rank highest

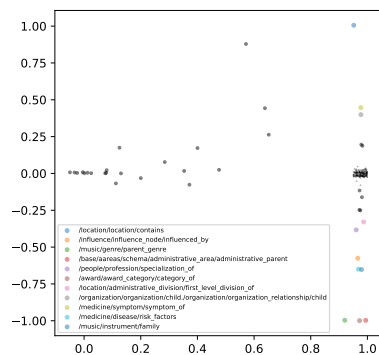


(a) Hierarchical-ness score visualization for all relations.

Relation	Score	Hierarchical
<i>source-UMLS:rel-name-PAR</i>	2.0	true
<i>source-MESH:rel-name-parent</i>	2.0	true
<i>source-DISGENET:rel-name-dis-gene</i>	2.0	true
<i>source-GO:rel-name-is_a</i>	2.0	true
<i>source-GO:rel-name-part_of</i>	2.0	true
<i>source-CLASSFIRE:rel-name-is_a</i>	2.0	true
<i>source-DRUGBANK:rel-name-parent</i>	2.0	true
<i>source-DRUGBANK:rel-name-other</i>	1.2	true
<i>source-CTD:rel-name-increases</i>	< 1.1	false
<i>source-CTD:rel-name-decreases</i>	< 1.1	false
<i>source-CTD:rel-name-affects</i>	< 1.1	false
<i>source-DRUGBANK:rel-name-inhibitor</i>	< 1.1	false
<i>source-DRUGBANK:rel-name-substrate</i>	< 1.1	false
<i>source-DRUGBANK:rel-name-agonist</i>	< 1.1	false
<i>source-DRUGBANK:rel-name-antagonist</i>	< 1.1	false
<i>source-DRUGBANK:rel-name-inducer</i>	< 1.1	false
<i>rest of the relations</i>	< 1.1	false

(b) Relation type classification based on Hierarchical-ness score.

Figure 9: Results on GO21 dataset. (a) Score (*asymmetry, tree_likeness*) as (x, y) coordinate in visualization. Orange dots denote hypernym type relations, violet dots denote hyponym type relations and black dots denote non-hierarchical relations. (b) Relations above the line are predicted to be hierarchical relations, and ground-truth relation type are in the third column. All relations are correctly predicted.



(a) Hierarchical-ness score visualization for all relations.

Relation	Score	Hierarchical
<i>administrative_area/administrative_parent</i>	2.0	true
<i>award_category/category_of</i>	2.0	true
<i>music/genre/parent_genre</i>	2.0	true
<i>location/contains</i>	2.0	true
<i>music/instrument/family</i>	1.7	true
<i>medicine/disease/risk_factors</i>	1.7	unknown
<i>influence/influence_node/influenced_by</i>	1.6	unknown
<i>medicine/symptom/symptom_of</i>	1.4	unknown
<i>organization_relationship/child</i>	1.4	true
<i>administrative_division/first_level_division_of</i>	1.3	true
<i>rest of the relations</i>	< 1.1	false

(b) Relation type classification based on Hierarchical-ness score.

Figure 10: Results on FB15k-237 dataset. (a) Score (*asymmetry, tree_likeness*) as (x, y) coordinate in visualization. Dots with non-black colors denote top hierarchical-like relations among all 237 relations (their meanings are annotated in lower left of the figure). (b) Relations above the line are predicted to be hierarchical relations, and ground-truth relation type in column 3 are manually labeled.

on Hierarchical-ness score and discover that they are indeed hierarchical relations (suggested by keywords in their name, such as “child”, “parent”).